Materials Research Express

PAPER

# Characterization and mechanical properties of sisal fabric reinforced polyvinyl alcohol green composites: effect of composition and loading direction



Materials Research Express

PAPER

# Characterization and mechanical properties of sisal fabric reinforced polyvinyl alcohol green composites: effect of composition and loading direction

RECEIVED
21 May 2019

REVISED
23 October 2019

ACCEPTED FOR PUBLICATION
12 November 2019

PUBLISHED
21 November 2019

Nagamadhu M[1,2], Jeyaraj P[2,3] and G C Mohan Kumar[2]

[1] Department of Mechanical Engineering, Acharya Institute of Technology, Bengaluru, Karnataka-560107, India
[2] Department of Mechanical Engineering, National Institute of Technology Karnataka, Surathkal, Srinivasanagar-575025, India
[3] Author to whom any correspondance should be addressed.

**E-mail:** pjeyaemkm@gmail.com

**Keywords:** woven sisal fabric, fabric properties, polyvinyl alcohol, mechanical properties.

## Abstract

This research focuses on microstructure characterization and exploring mechanical properties of sisal fabric reinforced Polyvinyl Alcohol composites using conventional vacuum-assisted pressure compression method. Naturally available sisal fiber is used as reinforcement material in this composite because of its abundant availability in Southern India. The sisal fiber, PVA and its composites were characterized using Fourier Transform Infrared Spectroscopy. Initially, Polyvinyl Alcohol polymer was cross-linked with Glutaraldehyde, and mechanical properties were evaluated. It was observed that 20% Glutaraldehyde and 80% Polyvinyl Alcohol polymer combination yielded best mechanical properties. Further, two plain and one weft rib were considered and their textile properties were characterized. The results revealed that fabric crimp and yarn linear density had significant influence on tensile properties of the fabric. Influence of different fabric properties such as weaving pattern, grams per unit area, and loading direction on mechanical properties of composites were analyzed. The woven fabric having least gram per unit area of sisal resulted in best mechanical properties like tensile, bending, and impact. The weft rib fabric composites in weft direction exhibited best mechanical properties.

## 1. Introduction

Now a day's natural fiber reinforced composites are used in many of the industrial applications as an alternative to conventional metallic materials because of their lightweight [1]. In partially, synthetic fiber reinforced composites are replaced by low density, high specific strength, modulus and relativity non-abrasive, biodegradable, eco-friendly natural plant-based fiber composites materials [2–4]. The factor behind this increased usage of natural fiber is due to the special interests in reducing the environmental effects by polymers and their composites. This also reduces the pressure due to the dependence on petroleum products.

Processing of plant-based natural fiber composites have issues like fiber alignment, resin rich area due to short and random reinforcement. In case of short natural fiber composites, fibers are cut into small length to get uniform mixing and distribution during its preparation. However, this reduces the strength of the composites; this can be overcome by using woven fabric reinforcement. However, in woven fabric composites, fabric properties play a major role in composites mechanical properties. Most of the reinforcements in composite material have a close relation with textile materials and textile forms especially when the fibrous reinforcement is concerned.

However, it also depends on the type of fiber, woven structures, yarn direction and its strength, the weight of the fabric and its volume fractions [5–7]. In the mid-twentieth century onwards fabric composites and modern polymers enabled the fabrication of performance geo-textiles and specialized textile products for the civil, automobile, aeronautical and marine engineering industries [8, 9]. However, many researchers exhibited that woven composites are promising mechanical properties and dynamic mechanical properties also ease during processing of composites [10]. Özdemir *et al* [11] investigated the tensile strengths of the certain cellular woven

fabrics compared with those of the plain woven fabric. They observed that plain woven fabric performed better during tensile tests than other cellular woven fabric. Pothan *et al* [12] investigated the effect of weave architecture on the ultimate mechanical properties of plain, twill and matt woven sisal fiber reinforced polyester composites prepared by the resin transfer molding technique. They observed that while the tensile strength showed an improvement by 52%, the tensile modulus gave an improvement of 100% in the case of composites with mat-weave architecture.

The use of sisal fiber composites can be found in engineering applications such as automobile due to their stability, strength, and availability [13, 14]. Qi *et al* [15] also studied cushioning properties of sisal fiber-starch composites and observed that the composite with 4:13 mass ratio of fiber and thermoplastic starch (TPS) exhibit the optimal cushioning property. These literature encouraged moving towards the sisal fiber and also as it possesses very good mechanical properties, also it's an alternative for jute, wood, hemp, banana composites.

The environmental hazards have been caused due to rapid industrialization and non-recycling of industrial wastes. The synthetic fibers also contribute for the industrial wastes which cannot be recycled and are non-biodegradable. In lieu of this, research on bio-degradable and bio-compatible polymer materials are identified as a one of the promising areas. The sisal fiber Polyvinyl alcohol (PVA) and Poly lactic acid (PLA) have exhibited moderate mechanical strength producing eco-friendly products with enhanced thermal stability by blending. Many researchers worked on PVA-based materials for packing industries, biomedical implants, civil and structural applications [16, 17]. PVA is one of the potential polymer as it has favorable biodegradable characteristics. However, the application of PVA materials is limited due to its high cost and slow degradation process especially under anaerobic condition [18]. The PVA and its blending materials also gives better mechanical properties upon reinforcing with the natural fiber and particles [19–21].

The strength of composite materials mainly depends on reinforcement material's properties and this paper focuses on to study the influence of woven fabric reinforcement in a polymer composite. In case of woven fabric, the major influencing fabric properties are woven structure, and gram per unit area (GSM) in addition to cover factor, crimp, number of warp, and weft yarns and mechanical properties of the fabrics. However, many researchers have worked on the effect of a gram per unit area of woven materials [5, 22] and weight fraction [23, 24] of woven fabric in composites. However, , limited literatures are available for the influence of cover factor of fabric, crimp, yarn linear density, number of warp and weft yarns and mechanical properties of fabric on composites. Further, it is evident that fabric reinforced composites are having better mechanical properties compared to typical short and random fiber composites because of the structural integrity of fabric orientation. In addition to that researchers are promoting and shifting towards bio-degradable polymer in addition to the bio-degradable reinforcement materials like natural fiber. Crystallinity of PLA matrix increases with sisal fiber content and sisal fibers acted as a nucleating agent. The major constituent in natural fibers is cellulose which acts as the reinforcing material in the cell wall. The cellulose molecules are laid down in micro-fibrils in which there are extensive hydrogen bondings between cellulose chains, producing strong crystalline structures. Much work has been published on the characterization of the hydrogen bonds in cellulose by using various methods, among which Fourier Transform Infrared Spectroscopy (FTIR) has proved to be one of the most useful technique [25–27]. In view of this, polymer and reinforcement material compound identification is very important to understand the chemical structure of composites.

This paper focused on preparation of woven sisal fabrics and its physical and textile characterization in both warp and weft directions. Further, these fabrics are used as a reinforcement material for Polyvinyl Alcohol polymer composites by varying fiber weight fraction. The chemical compositions of sisal fiber, polymer and its composites were studied to understand the effect of chemical structures. The mechanical properties of cross linked Polyvinyl Alcohol in Glutaraldehyde were studied by varying weight percentage. Further, the optimal cross linked polymer was used to prepare the composites. The effect of GSM and woven pattern were studied in both warp and weft directions by understanding the influence of fabric physical properties.

## 2. Materials

### 2.1. Matrix materials

Polyvinyl Alcohol (PVA) and Glutaraldehyde (GA) are procured from M/s. Leo Chem India, Bengaluru, India. PVA $(CH_2CH(OH))_n$. used as biodegradable matrix material [18, 19] and has a molecular weight of 85 000 to 124 000 with a degree of hydroxylation varying from 87 to 89. The molar mass of PVA and GA are 44.05 and 100.12 g $mol^{-1}$ respectively. The viscosity of 4% aqueous solution at 20 °C is varies from 23 to 38 cps. pH varies from 4.5 to 6.5 and has an ash content maximum of 0.75%. The melting point and boiling points are 200 °C and 228 °C respectively. The density of PVA is 1.19 g $cm^{-3}$. Glutaraldehyde $(OHC(CH_2)_3CHO)$ is a 25% aqueous solution which is having a density of 1.06 g $cm^{-3}$.

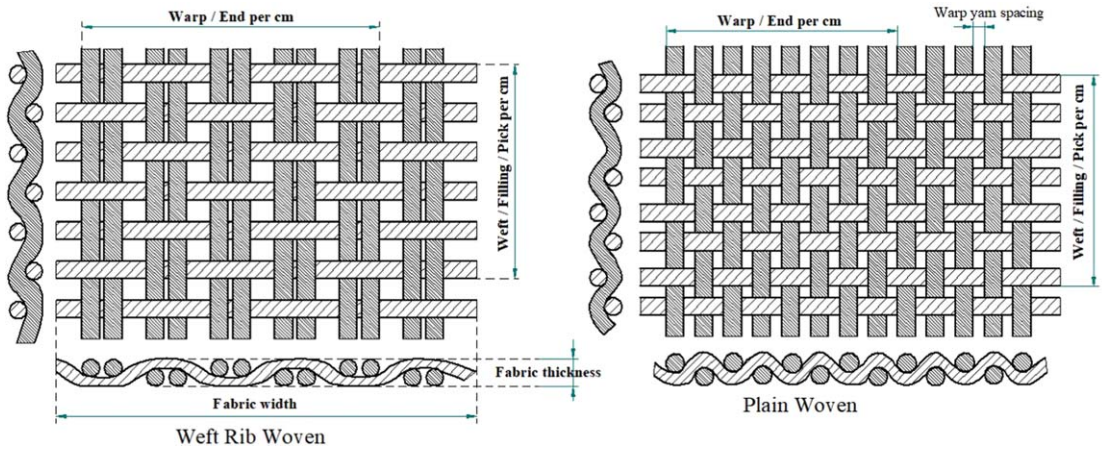


**Figure 1.** Schematic diagram of plain and weft rib woven fabrics and cross-section views.

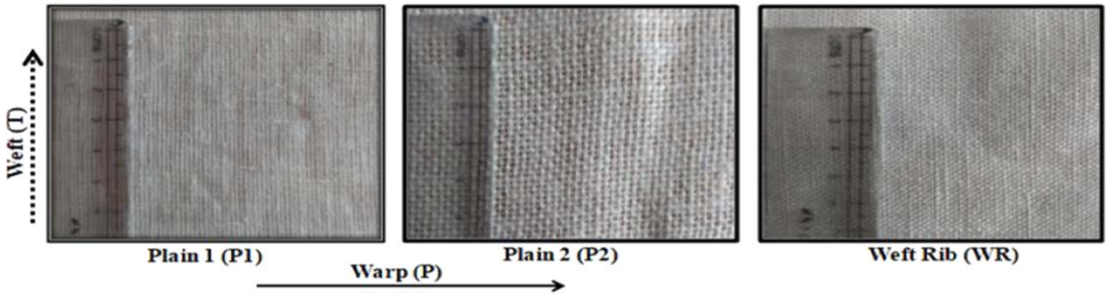


**Figure 2.** Plain and weft rib woven sisal fabrics.

**Table 1.** Standard methods used to determine different fabric properties.

| Methods | Properties | Testing | Standard method |
|---|---|---|---|
| Yarn Testing Methods | Yarn crimp | Yarn crimp and yarn take-up in woven fabrics | ASTM: D3883 |
| | Yarn size | Yarn number (linear density) | ASTM: D1907 |
| Fabric Basic Properties Testing Methods | Fabric density | Warp (end) and filling (pick) count of woven fabrics | ASTM: D3775 |
| | Fabric weight | Mass per unit area of fabric | ASTM: D3776 |
| | Fabric thickness | Thickness of textile materials | ASTM: D1777 |
| Fabric Mechanical Properties Testing Methods | Tensile Strength | Fixing fabric two ends | IS: 1969–1985 |

### 2.2. Reinforcement material

Sisal fibers are extracted from the plant leaves obtained from the district of Karnataka state, India and washed [28]. These sisal fibers are converted in to yarn and then fabric at M/s. OM Textile Industries, Bengaluru, India. Two woven sisal fabric are prepared by maintain same woven structure (Plain) and with varied gram square meter (GSM) designated as Plain 1 (P1) and Plain 2 (P2). One Weft Rib (WR) sisal woven fabric was also prepared. This also comes under the category of plain woven structure, but two weft yarns are crossed with one warp yarns. Figure 1 shows the schematic picture of the plain and weft rib weave fabric structure, whereas figure 2 shows the view of P1, P2 and WR woven sisal fabrics used in this work.

These sisal woven fabrics are tested according to textile materials test standards as shown in table 1 at Department of Fashion and Apparel Design, Acharya Institute, Bengaluru and Central Silk Technological Research Institute, Bengaluru, India.

### 2.3. Processing of composites

Polyvinyl Alcohol and 20% of Glutaraldehyde mixed and sisal woven fabrics are used to prepare composites by using conventional vacuum-assisted pressure compression method. Figure 3 shows the schematic diagram of

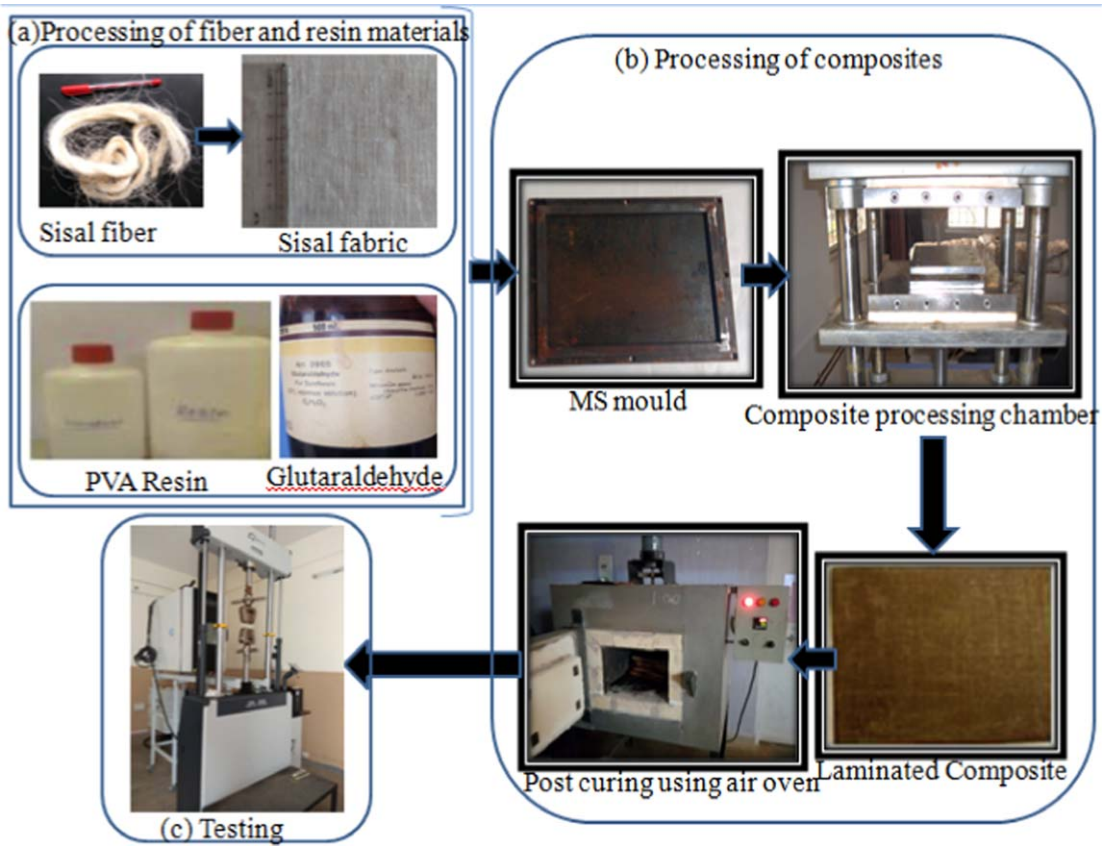


**Figure 3.** Schematic representation preparation steps of woven sisal fabric composite.

steps involved from extraction of sisal fiber to testing of composites. Figure 3(a) shows extracted sisal fiber and then converted into woven sisal fabrics. The resin and fabric materials are loaded into MS mold having mold dimensions of 250 × 200 × 4 mm and kept in the vacuum-assisted pressure compression method shown in figure 3(b). The prepared laminated composites are post-cured for 24 h at 60 °C using conventional air oven, and then treated with 2 mole of Sulfuric acid ($H_2SO_4$) for 24 h for complete cross-linking. The samples were prepared as per ASTM standards and their compositions are abbreviated and are shown in table 2. Figure 3(c) represents the universal Testing Machine (UTM) which is used to determine the mechanical properties of composites.

## 3. Testing standards/methods

### 3.1. Fourier transform infrared spectroscopy

In order to identify the organic and polymeric compounds the Perkin Elmer Fourier Transform Infrared Spectroscopy was used. In which Frontier Optica model was preformed to measure the PVA [29, 30], Sisal fiber and its composites at highest accuracy. All samples were completely dried to avoid unwanted peaks [31]. Then, the FTIR spectroscopy was recorded by accumulating 16 scans at 4 $cm^{-1}$ resolution between 500 $cm^{-1}$ to 4000 $cm^{-1}$ range.

The sisal fiber chemical compositions were analyzed at M/s. Intertek Testing Services India Pvt Ltd, Bengaluru, India.

### 3.2. Characterization of yarn

Yarn properties like linear density and crimp are directly influenced to the strength of the composites [32]. These studies by unravel yarn from the fabric and then cut into 1 m length and it was weighed using a weighing balance. Yarn linear density was measured by averaging ten samples reading according to ASTM: D1907 in tex.

The yarn crimp measured according to ASTM: D3883. The yarn length was measured in the fabric (Length of yarn in the fabric - $Y_1$), then yarns are unraveled from the fabric and measured the length of the yarn without exerting extreme force - $Y_2$. The yarn crimp, C, was calculated using the relation.

**Table 2.** The composition of composites and their representation.

| Sl No | Material | Composition of fabric | Loading directions | Representations of samples |
|---|---|---|---|---|
| 1 | Neat Sample (PVA and 20% GA) | 0 | Neat resin | PVA- 20GA |
| 2 | Plain 1 (P1) | 20% | Warp | P1–20-P |
| 3 | | | Weft | P1-20-T |
| 4 | | 40% | Warp | P1-40-P |
| 5 | | | Weft | P1-40-T |
| 6 | | 60% | Warp | P1-60-P |
| 7 | | | Weft | P1-60-T |
| 8 | Plain 2 (P2) | 20% | Warp | P2-20-P |
| 9 | | | Weft | P2-20-T |
| 10 | | 40% | Warp | P2-40-P |
| 11 | | | Weft | P2-40-T |
| 12 | | 60% | Warp | P2-60-P |
| 13 | | | Weft | P2-60-T |
| 14 | Weft Rib (WR) | 20% | Warp | WR-20-P |
| 15 | | | Weft | WR-20-T |
| 16 | | 40% | Warp | WR-40-P |
| 17 | | | Weft | WR-40-T |
| 18 | | 60% | Warp | WR-60-P |
| 19 | | | Weft | WR-60-T |

$$Yarn\ Crimp(\%)C = [Y_2 - Y_1/Y_1] \times 100 \quad (1)$$

In case of plain woven pattern the weave repeats on two warp and two weft. It gives maximum number of interlacement in the fabric and therefore the fabric becomes very stiff. In case of plain woven pattern weft undergoes more number of interlacement than the warp direction, therefore the crimp in the weft yarns is higher than the warp yarns as shown in table 3. In case of weft rib the warp yarns undergoes more number of interlacement than the weft yarns and therefore the crimp in the warp yarns is higher than that of weft yarns.

### 3.3. Characterization of fabric

The fabric physical properties like yarn density (fabric density), mass per unit area and thickness are also having a significant impact on mechanical properties of composites. The yarn spacing refers to the compactness of fabric is called as fabric density and it is measured according to ASTM: D3775.

The fabric weight was measured in grams per unit area (GSM) ($g/m^2$) and fabric thickness was measured using Askhi fabric thickness indicator which was having least count of 0.01 mm according to ASTM: D1777. These properties for three different fabrics are measured and given in table 3. The influence of these properties on mechanical properties of fabric, and composites were explained in detail in the section 4.

Tensile properties of the fabric such as ultimate load, ultimate point extension, ultimate stress, ultimate point strain, young's modulus, breaking point load and breaking point extension obtained according to textile testing standards by averaging ten identical samples. Tensile properties of sisal fabrics were measured acceding to IS: 1969–1985 in both warp and weft directions using universal Testing Machine (UTM). The samples are fixed such a way that load equality distributed on each yarn by maintaining gauge length of 200 mm, and width 50 mm, crosshead speed 3 mm $min^{-1}$.

### 3.4. Mechanical properties of composites

The tensile strength was determined according to ASTM D638–03 with samples of size dimensions of 160 mm length, 12.5 mm width and 4 mm thickness. The tensile test was conducted at a rate of 10 mm $min^{-1}$ with a gauge length of 100 mm. Flexural tests were conducted according to ASTM D790 standard using samples with a width 12.7 mm, length 127 mm, and thickness 4 mm, with a crosshead speed of 2 mm $min^{-1}$ and a span length of 90 mm. The impact test was conducted using Izod Impact tester according to ASTM D 256 standard and a sample with dimensions of width 12.7 mm, length 64 mm, and thickness 4 mm. These mechanical properties of resin and composites were evaluated based on the average value of tests conducted on five identical samples.

### 3.5. The microstructure of fractured surface

The microstructures of sisal fabric composite were analyzed to understand the influence of textile microstructure on mechanical properties. Also, the interfacial bonding between the matrix and fabric material were studied using Scanning Electron Microscopy (SEM) images.

**Table 3.** Textile properties of different fabrics.

| Sl. No | Woven type | Fabric thickness in mm | GSM | Cover factor (%) | | Yarn Count in Tex | | Yarn crimp (%) | | Number of yarns per cm | |
|---|---|---|---|---|---|---|---|---|---|---|---|
| | | | | Warp (**P**) | Weft (**T**) | Warp (**P**) | Weft (**T**) | Warp (**P**) | Weft (**T**) | Warp (**P**) | Weft (**T**) |
| 1 | **Plain 1** | 0.42 | 161.02 ± 0.17 | 79.18 ± 0.46 | 91.78 ± 0.69 | 80.1 ± 0.56 | 85.1 ± 1.67 | 7.23 ± 0.26 | 9.54 ± 1.12 | 18 ± 0.95 | 20 ± 1.06 |
| 2 | **Plain 2** | 0.73 | 296.60 ± 1.75 | 74.28 ± 2.80 | 80.24 ± 3.75 | 182.3 ± 4.43 | 166.8 ± 8.41 | 6.53 ± 0.97 | 11.06 ± 1.09 | 12 ± 0.74 | 12 ± 0.67 |
| 3 | **Weft rib** | 0.72 | 300.45 ± 1.67 | 82.12 ± 3.09 | 53.01 ± 3.06 | 65.3 ± 2.51 | 182.9 ± 4.04 | 10.05 ± 0.94 | 5.96 ± 1.22 | 22 ± 1.03 | 11 ± 1.05 |

Standard deviations are in (±) for 10 trials.

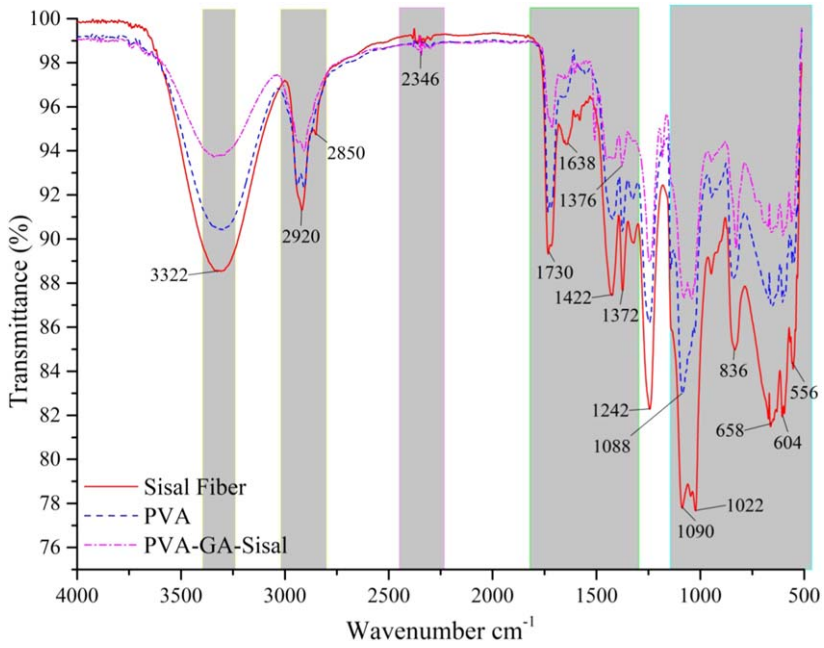


**Figure 4.** FTIR spectra of PVA, sisal fiber and its composites.

## 4. 4. Results and discussions

### 4.1. Fourier transform infrared spectroscopy analysis

The FTIR is considered as an important technique for getting information about the specific groups in the compositions as well as the interaction between the PVA, sisal fiber and its composites. Each material has a characteristic band predominate in the interaction. Figure 4 shows the spectra of FTIR for sisal fiber exhibit strong broad peaks range from 3300 $cm^{-1}$ to 3500 $cm^{-1}$ [33] demonstrates O–H stretching of the hydroxyl group in the lignin and cellulosic structure and a peak at 1638 $cm^{-1}$ is due to the characteristic axial vibration of hydroxyl group O–H of cellulose. The small peak around 1590 $cm^{-1}$ is attributable to the out of plane bending of NH [34]. The strong peak between 2900 $cm^{-1}$ to 3950 $cm^{-1}$ related to C–H stretching of cellulose component, this is due to the aliphatic saturated C–H stretching vibration in cellulose and hemicelluloses form $–CH_2$. The wave number 2920 $cm^{-1}$ also corresponds to the stretching vibration of $CH_2$ groups, while peak at 1422 $cm^{-1}$ can be interpreted as deformation vibrations of the same group. In addition, –C–H stretching at round 2900 $cm^{-1}$ also observed in sisal fiber spectra [33]. According to Namrata *et al* [35] the 1720 $cm^{-1}$ to 1740 $cm^{-1}$ attributed to C=O unconjugated stretching of the ester linkage of carboxylic group of the ferulic and *p*-coumaric acids of lignin of the residual hemicelluloses. The small peak 1638 $cm^{-1}$ assigned to O–H bending due to absorption of water/moisture content in the sisal fiber. The peak at 1422 $cm^{-1}$ and 900 $cm^{-1}$ are assigned to $CH_2$ symmetric bending of crystalline cellulose and the cellulosic $\beta$-glycosidic linkage. The peak 1372 $cm^{-1}$ attributed to in-the-plane –C–H bending vibration. The peak 1242 $cm^{-1}$ presence of both lignin and pectin attributed to C–O ring of lignin. The peak 1242 $cm^{-1}$ indicates lignin assigned to C–O stretching vibration of acyl group present in the lignin. Asha *et al* [36] identified the peak line between 1100–1160 $cm^{-1}$ assigned to C–O–C stretching vibration and hydrogen bonded / ether linkage (C–O–C) form lignin or hemicelluloses. The band at 1088 $cm^{-1}$ is due to the associated hydrogen group and the small band peak also observed at around 1045 $cm^{-1}$ denotes C–O band of the primary and secondary hydroxyl group in the cellulose, lignin and their glycoside linkages in the sisal fiber. Rajashekaran *et al* [37] reported that peak around 1,660 $cm^{-1}$ correspond to –C=O stretching due to the presence of aliphatic carboxylic acid in cellulose chain.

In the spectrum of PVA a broad peak seen at 3322 $cm^{-1}$ attributed to the OH group. The peak at 1645 $cm^{-1}$ corresponds to the carbonyl group and the peak 1539 $cm^{-1}$ indicates the OH vibration. The characteristic band seen at 1732 $cm^{-1}$ indicates the carboxylic (C=O) stretching and C–O stretching corresponding to alcohol groups were observed at 1246, 1088, 840 $cm^{-1}$ and 607 $cm^{-1}$ [38]. The peaks at 2910 $cm^{-1}$ indicate the C–H stretching and the peaks at 1377 $cm^{-1}$ indicate the C–H group [39]. The broad absorption bands at 1088 $cm^{-1}$ indicate the C–O stretching. C–H group vibration peaks were observed at 1240 $cm^{-1}$ and around 1323 $cm^{-1}$. Other groups at 1158, 929, and 835 $cm^{-1}$ attributed, respectively, to C–O–C, C–C, and H–C–H stretching

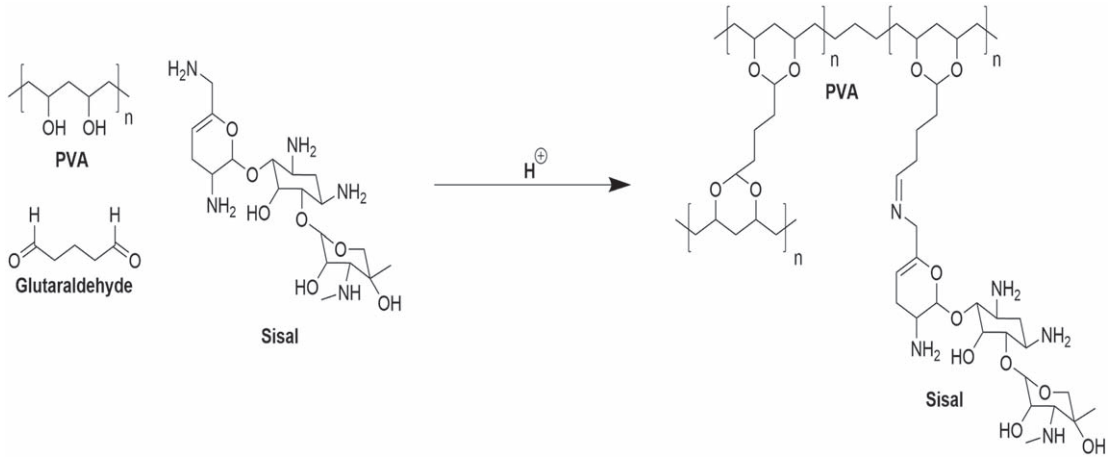


**Figure 5.** Chemical structure of PVA, GA and its composites and reactions.

modes. The IR spectra of PVA-GA-sisal composite shows the improvement in the peaks and based on group identifications the chemical structures of PVA, GA, Sisal fiber [40] and its composite were drawn shown in figure 5.

Further the cross sections of single sisal fiber were analyzed using SEM analyzed and shown in figure 6(a). The chemical composition of extracted sisal fiber which is available in Karnataka, India has 62%-76% cellulose, 23%-36% hemicelluloses, 6%-9% lignin, 0.8%–1.3% wax and 5%–10% moisture. The average diameters of the sisal fiber were found to be varying from 100 to 350 micrometers shows in figure 6(a). The sisal fiber available in various parts of India was compared from the literatures. Khan *et al* [41] reported that sisal fiber which is available in Bhopal has 77%–85% homocellulose, 65%–73% cellulose, 9%–11% hemicelluloses, 5%–6% lignin, 0.9%–1.2% wax and 9%–11% moisture. Sreekumar *et al* [42] studied the southern part of Indian sisal fiber which is available in Kerala region and found that 100–300 μm diameter, 1.450 g $cm^{-2}$ density, 65%–78% cellulose, 10%–14% hemicellulose, 10% Pectin, 9.9% Lignin, 2% Waxes. Maya *et al* [43] studied sisal fiber Kerala state which is contain 78% cellulose, 10% hemicelluloses, 8% lignin, 2% wax, and 1% ash. Similarly, chemical composition of sisal fiber reported by Favaro *et al* [44] that sisal fiber has 43%–56% cellulose, 21%–24% hemicelluloses, 7%–9% lignin, 0.6%–1.1% ash. Franklin *et al* [45] observed that sisal fiber has 6.27% moisture, 1.20% Ash, 1.75% Extractives, 31.81% Hemicellulose, 11.07% Lignin, 48.20% Alpha cellulose.

### 4.2. Characterization of fabric

Figure 7 shows a typical tensile stress-strain curve for the sisal fabric used in this study. The initial part of the curve is nonlinear then its slope has increased slowly until the fabric fails. It is difficult to determine the mechanical properties of the sisal fabric by taking nonlinear curve into consideration [26]. Hence, a linear extension as shown in figure 7 was constructed for the linear part from the strain axis. With this linear extrusion, for each stress-strain curve, the tensile modulus and ultimate tensile stress and strain at peak could be determined.

The investigation carried out on the woven sisal fabric for the evaluation and understanding of behavior under tensile loading can be clustered into three phases as shown in figure 7. The phase one was the initial region that exhibits a curve with a lesser slope. The phase two was the linear region of the curve after the fabric settlement, which rose steadily till it reached it's peak and the phase three was the part of the curve after it reaches the peak. In the initial phase, the curve rose with a low slope due to decrimping and crimp interchange. The decrimping and crimp interchange was an internal interaction (crossover between warp and weft yarns) of a fabric that results to the initial curve. When a woven sisal fabric was stretched in its principal directions, a straightening of the crimped yarns occurred in the direction of the load. In the direction of load, the yarns appear to become less flattened due to the consolidation into more circular cross-section. As the stress built up for the yarn in the direction of load, the continuous interchange between two yarns also happened simultaneously thus increases the crimp in the yarn perpendicular to the loading direction.

Yarns along the direction of the load would continuously become round and less flattened as the fabric was further extended. Here, yarn and fiber extensions occurred, but the yarn extension only accounts for a small portion as compared to the extension in yarn in the phase one. The small extension of yarn suggests that the interaction between the fibers due to the twist given to the yarn become tighter and stronger and increase the

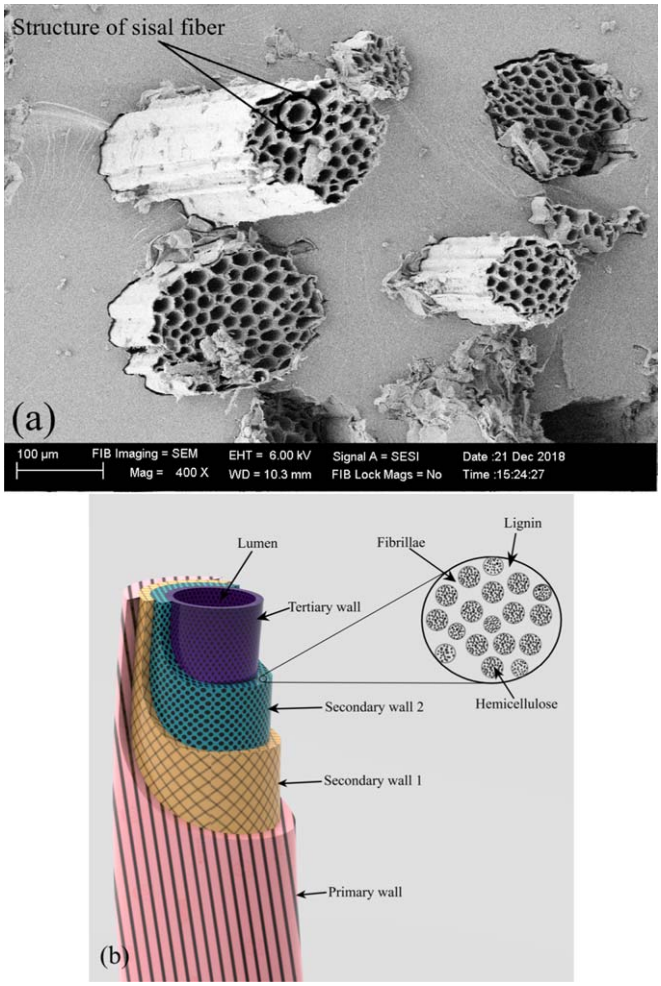


**Figure 6.** (a) Cross section of sisal fibers (b) Structure of sisal fiber.

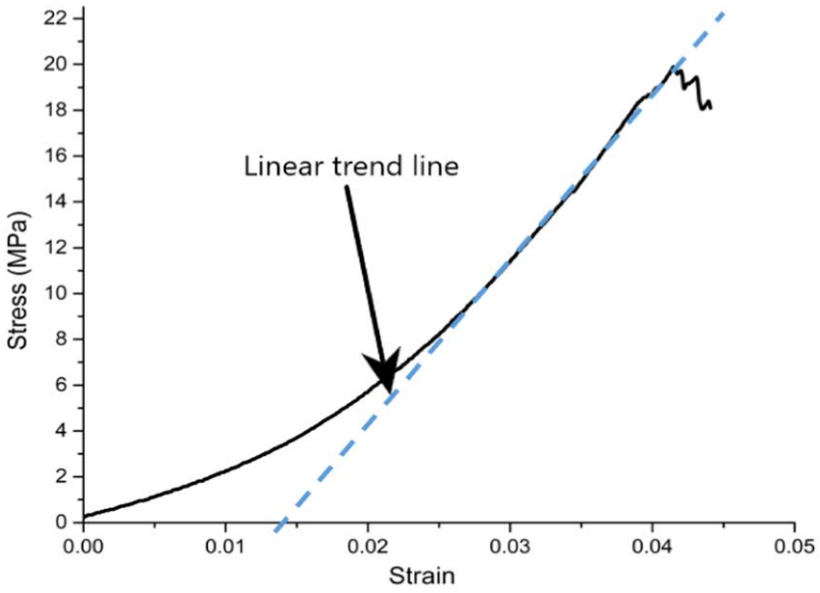


**Figure 7.** The typical tensile stress-strain curve of sisal fabric.

stress for the yarn to resist tensioning load. The internal interaction still happened, but the contribution of the perpendicular yarns against the loading direction was just small. This behavior is shown in the phase two in which the load-extension curve increased sharply until it reached the peak and then broken down of yarns.

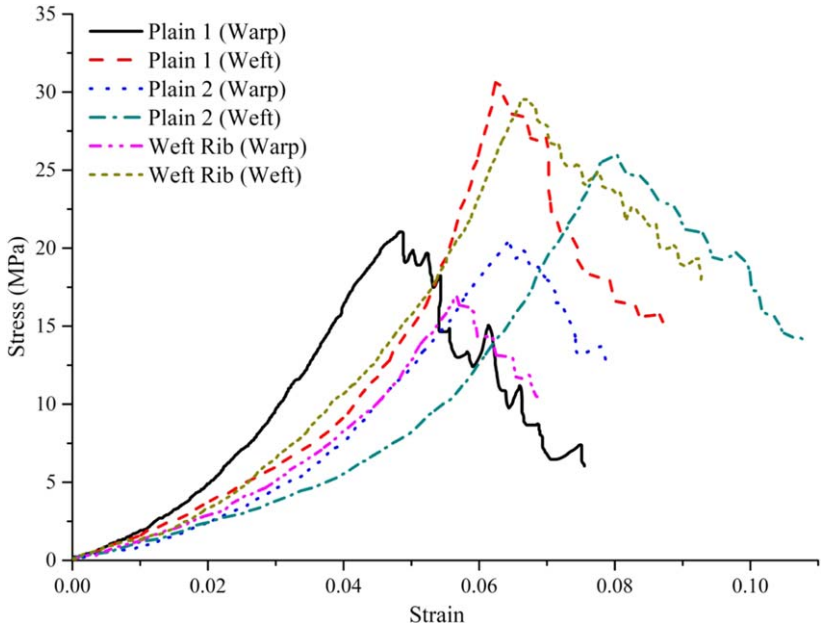


**Figure 8.** Tensile stress-strain curves for fabrics in weft and warp directions.

The stress-strain responses of different fabrics under tensile loading are shown in figure 8. For each fabric, the specimens were cut and tested for the loading on warp and weft directions. The tensile properties were measured at the maximum stress or ultimate stress and the corresponding elongation noted to find strain at an ultimate point.

Figure 8, shows the stress-strain curves for loading along warp and weft direction for all the fabrics considered. Table 4 shows the summery of fabric tensile results and its standard deviation for ten trials. In P1 type of fabric weft direction exhibit better ultimate tensile strength (1.36 times) and higher strain value (1.42 times) then the warp direction. This increase in the ultimate tensile strength depends on yarns count, more in weft (85.1) as compared to warp (80.1). The higher strain can be attributed to higher yarn crimp percentage associated with the weft direction. The similar trend observed in P2 woven fabric, weft direction exhibit better ultimate tensile strength (1.1 times) and higher strain value (1.23 times) then the warp direction. However, the yarn count is 166.8 in weft which was little lesser then warp, even though ultimate tensile stress was more in weft as compared to warp. This was mainly due to the textile fabrication. The same observation was also noticed for plain hemp stress-strain graph in both warp and weft direction [46]. In comparison with P1 and P2, P2 fabric is having 1.81 times in warp and 1.45 times in weft load withstanding capacity. This clearly shows gram per unit area directly proportional to load carrying capacity and finer fabric with higher cover factor exhibit better tensile Modulus. In WR woven fabric the weft direction (1.6 times) shows better properties than the warp direction. This may be due to the influence of yarn density (fabric density). This could clearly show that woven structure properties of fabric also having a significant impact on tensile properties of the fabrics.

### 4.3. Mechanical properties of resin

Initially, a tensile and flexural property of the matrix materials is characterized to understand the effect of the influence of GA on PVA. The percentage of GA is varied from 0% to 40% in a step of 5% and corresponding variation in tensile and flexural properties are analyzed. Further, by considering the optimum percentage of GA and PVA the woven sisal fiber compositions were prepared for 20, 40 and 60% weight fraction of sisal fabrics. Plain 1 (P1) and Plain 2 (P2) composites were considered to study the effect of GSM of fabric on mechanical properties of the composite. Plain 2 (P2) and Weft rib (WR) composites were used to understand the effect of woven structures on mechanical properties of the composites. The representations of these composites and their abbreviation are shown in table 2.

#### *4.3.1. Tensile strength*

The tensile properties of resin were characterized as per ASTM D638–08 standard to understand the effect of GA in PVA. Figure 9 clearly shows that ultimate stress increases by adding GA up to 20 wt%, beyond 20% wt% the tensile strength observed to decrease. The better combination of PVA-GA is found at 20% with maximum

**Table 4.** Tensile properties of sisal fabric.

| Type of fabric | Directions | Ultimate Point | | Breaking Point | | Ultimate Point | | Tensile Modulus ($N/mm^2$) |
|---|---|---|---|---|---|---|---|---|
| | | Load (N) | Elongation (mm) | Load (N) | Elongation (mm) | Stress ($N/mm^2$) | Strain | |
| Plain 1 | Warp | 481.2 ± 21.5 | 9.67 ± 0.39 | 159.72 ± 83.5 | 14.74 ± 1.28 | 22.91 ± 1.02 | 0.048 ± 0.0019 | 474.743 |
| | Weft | 655.9 ± 13.1 | 13.51 ± 0.69 | 322.53 ± 39.0 | 20.24 ± 1.55 | 31.23 ± 0.62 | 0.068 ± 0.0034 | 463.237 |
| Plain 2 | Warp | 869.2 ± 31.0 | 12.88 ± 0.50 | 405.80 ± 79.3 | 19.14 ± 2.02 | 23.81 ± 0.85 | 0.064 ± 0.0025 | 370.233 |
| | Weft | 952.8 ± 8.0 | 15.85 ± 0.35 | 471.60 ± 72.8 | 21.55 ± 0.21 | 26.10 ± 0.21 | 0.079 ± 0.0018 | 329.419 |
| Weft Rib | Warp | 672.0 ± 48.2 | 11.02 ± 0.30 | 223.40 ± 98.4 | 14.77 ± 0.96 | 18.66 ± 1.34 | 0.055 ± 0.0015 | 339.405 |
| | Weft | 1074.5 ± 10.0 | 13.21 ± 0.18 | 421.81 ± 103.3 | 20.40 ± 1.21 | 29.84 ± 0.28 | 0.066 ± 0.0009 | 451.716 |

(±) standard deviation for ten tensile trials.

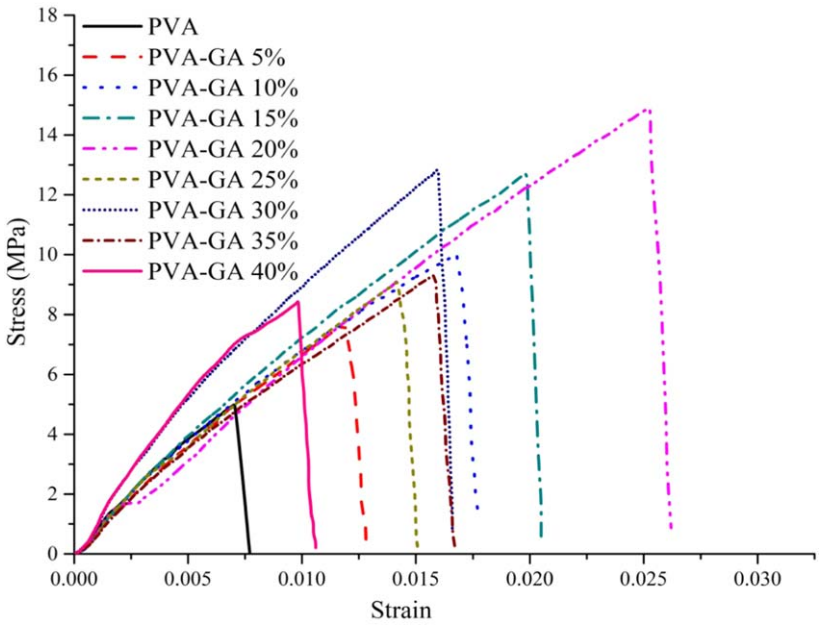


**Figure 9.** Tensile stress-strain plot for various percentage of GA in PVA.

tensile strength 14.96 MPa. The area under the curve represents the strain energy absorption of resin material found to highest at 20% GA due to the establishment of effective cross-linking. This also represents that the static toughness is highest for 20% of GA cross-linking beyond this wt % results in poor strength this may be due to improper bonding [47].

*4.3.2. Flexural strength*

The flexural properties of resin were characterized as per ASTM D790 standard to understand the effect of GA in PVA and results are given in figure 10. It clearly shows that load carrying capacity increases with the addition of GA. However, the same composition exhibiting favorable bending properties and allows deformation. Comparing to tensile testing behavior in flexural mode resin are exhibiting good ductility and energy absorption capability. The optimum combinations of GA in PVA were found to be at 20% even in a flexural mode.

### 4.4. Effect of GSM on mechanical properties of composites.

*4.4.1. Tensile properties*

Tensile behavior of P1 and P2 composites for various weight fractions of sisal fabric in warp and weft directions is analyzed and results are given in figures 11 and 12 respectively.

Figure 11, it is clear that the fiber weight fraction increases the ultimate tensile strength and strain of the composite. The ultimate tensile stress increases by 3.5 and 6.2 times for tensile loading in weft direction for adding 40 and 60% wt% of fiber. The ultimate stress found to be maximum in weft direction as compared to warp directions. In P1 type composites, the strain increases with increase in fiber loading; this may be due to the stretching behavior of fabric material. The tensile strains were found to be less in weft direction even though fabrics having higher strain values, this is due to the cover factor of the fabric. Cover factor of the fabric is lesser in warp direction which leads to resin rich. This is explained in detail using SEM images in section 4.5. As yarns are twisted and fibers in yarns are creating crinkles texturing the high degree of interface possesses between matrix to the fabric material. This clearly shows that energy absorption increases with fiber loading, the weft direction of composite exhibit better toughness as compared to warp direction. The increases in ultimate stress could be attributed to increase in surface area between woven sisal fabric and resin. This also attributed reference to figure 8, P1 type fabric having a better tensile strength in weft direction as compared to warp direction.

The ultimate tensile stress increased by 1.58 times in warp and 1.63 times in weft by adding 20% of P2 woven fabric which is less than that of P1. The same trend continues at higher percentage of fiber loadings also. This clearly shows that GSM of a fabric is having a significant effect on tensile properties. The strain values of the composite show higher in weft direction as compared to warp direction as already observed in textile tensile properties of the fabric. A comparison of P1 and P2 based composite, P1 based composite shows better ultimate tensile stress. This can be attributed to higher GSM value of P2 fabric compared to the P1 fabric [9]. However, in comparison, it is also observed that there is no significant change in strain at a lower percentage of fiber loading.

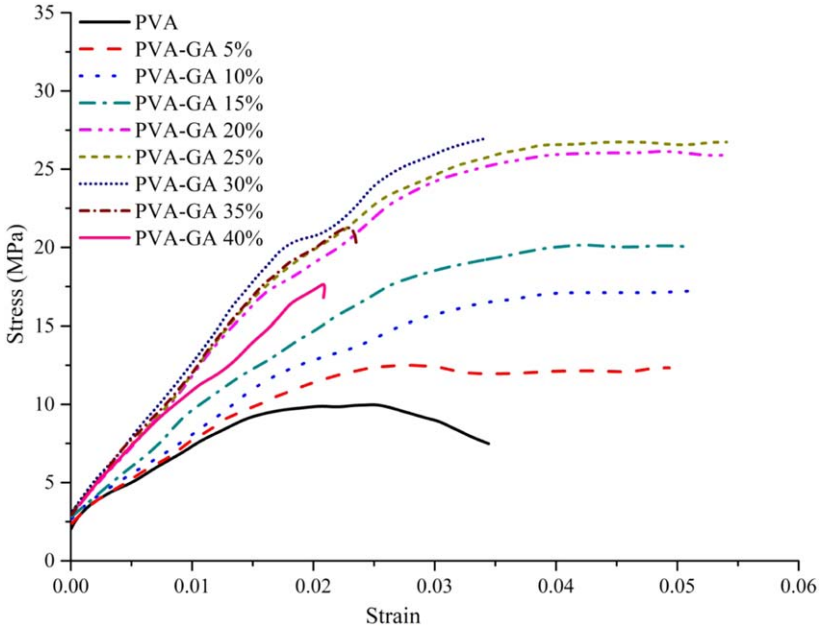


**Figure 10.** Flexural stress-strain plot for a various percentage of GA in PVA.

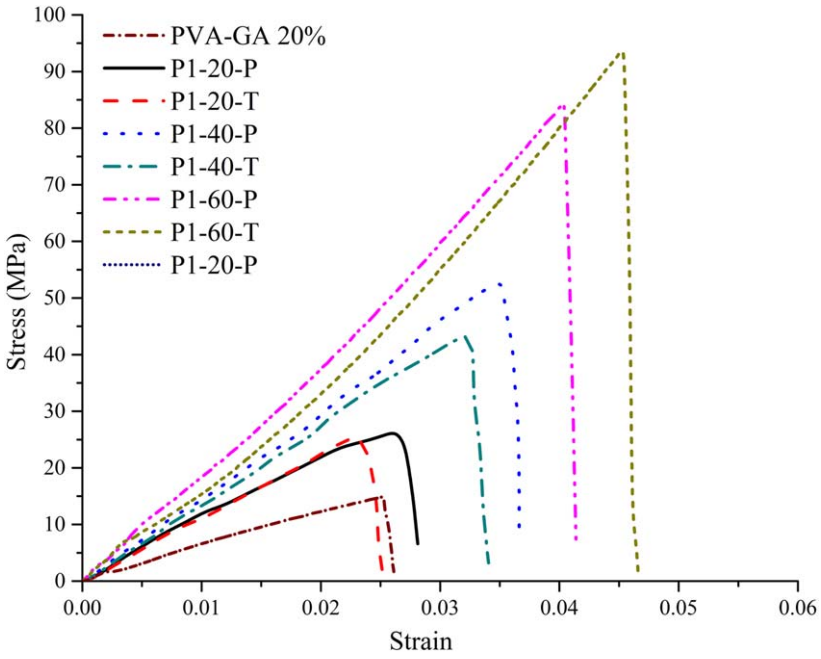


**Figure 11.** Tensile Stress-strain curves of Plain 1 composites for various weight fractions in both warp and weft directions.

But, P2 based composites show higher strain value (0.0552) at 60% fiber loading as compared to P1 (0.0454) this may be due to the yarn linear density and yarn count. This clearly shows that weft direction of composites possesses more energy absorption as compared to warp direction. It is also observed that strain energy absorption and toughness increases by increasing the fiber percentage in the composites. The nature of the curve was found to be brittle in both P1 and P2 based composites.

The tensile strength of both P1 and P2 based composites are higher than the untreated short (20 mm length) sisal fiber reinforced polypropylene composite fabricated by mini twin-screw extruder which is 40 MPa [48]. Asokan *et al* [49] also reported 30% weight fraction of short fiber (4 mm) sisal and hemp hybrid reinforced PLA composite fails at around 33 MPa which is lesser as compared to P1 and P2 based composite. Also tensile strain was found to be high in PVA matrix material. Saurabh *et al* [50] worked on cyclicality behavior of 30 weight

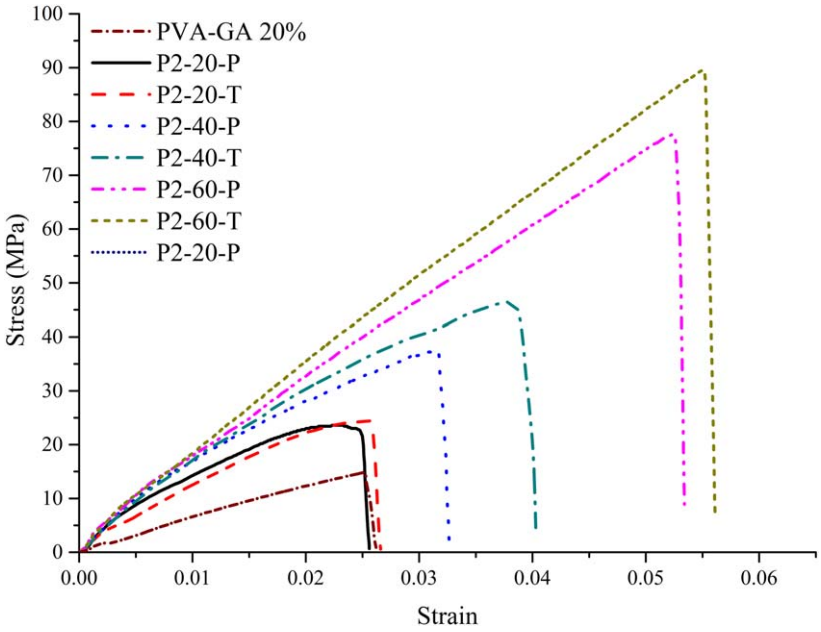


**Figure 12.** Tensile Stress-strain curves of Plain 2 composites for various weight fractions in both warp and weft directions.

fraction sisal fiber PLA composites using single screw extruder and observed that tensile strength of recycled PLA sisal fiber composites was around 50 MPa and further it's not recommended for structural applications. Rahesh *et al* [51] studied the effect of sisal fiber reinforcement and observed that tensile and bending strength increased by adding sisal fiber. Maya *et al* [43] also observed that sisal fabric reinforced natural rubber composites exhibit tensile strength of 22 MPa. Andressa *et al* [52] observed sisal fabric phenolic composite and found tensile strength and flexural strength are 25 MPa and 11 MPa respectively.

*4.4.2. Flexural properties*

Stress-strain response of the different types P1 and P2 composites under flexural loading is given in figures 13 and figure 14 respectively. Figure 13, it is clear that wt% of sisal fabric reinforcement enhances bending strength of the composite. Same trend has been observed for both warp and weft cases. However, weft direction of composite exhibit better flexural properties as compared to warp direction. The better load carrying capacity in weft direction is due to the higher yarn count and crimp percentage associated with weft direction as seen in table 3.

Influence of sisal fabric loading on strain-strain behavior of P2 composite under flexural loading is similar to the P1 composites as seen in figure 14. As compared to P1 based composite, P2 based composites having sight higher load bearing capacity but fails at less amount of strain. This clearly shows that yarn linear density and yarn count having a significant impact on flexural properties. The flexural behavior of P1 based composites are like ductile in nature, but in case of P2 ductile fracture are changed to brittle by reinforcing more amount of fiber to it.

The flexural strength of both P1 and P2 based composites are slightly less than the untreated short (20 mm length) sisal fiber reinforced polypropylene composite fabricated by mini twin-screw extruder with same weight fraction of fiber [48]. Asokan *et al* [49] also reported 30% weight fraction of short fiber (4 mm) sisal and hemp hybrid reinforced PLA composite is fails at around 155 MPa which is higher as compared to P1 and P2 based composite. The flexural strength was around 80 MPa after third recycling of PLA sisal fiber composites [50]. This may be due to the composite processing and the effect of reinforcement and matrix material.

*4.4.3. Impact strength*

Influence of fiber loading on impact strength of different composite analyzed is given in table 5. It is clear that impact strength is influenced by nature of fabric. P2 based composites exhibit better impact strength than P1 based composites. This clearly shows that the GSM of the fabric also influence the impact properties. The weft direction of composites exhibits better impact strength both P1 and P2 based composites compared to warp direction of composite. This may be due to the combined effect of cover factor and crimp.

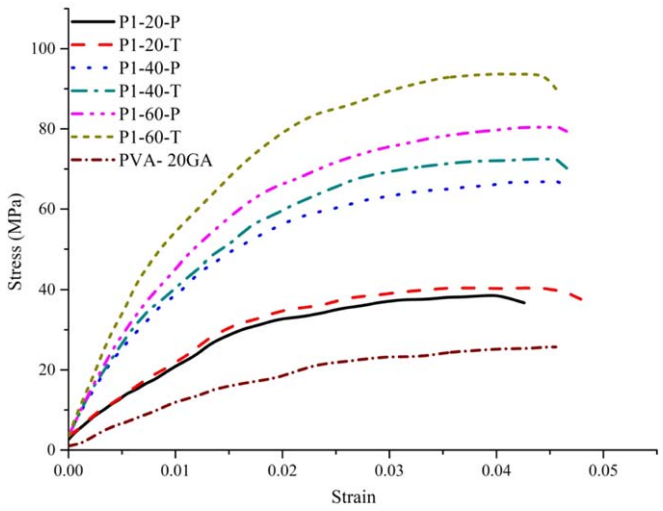


**Figure 13.** Stress-strain curves of Plain 1 composites for various weight fractions in both warp and weft directions under flexural loading.

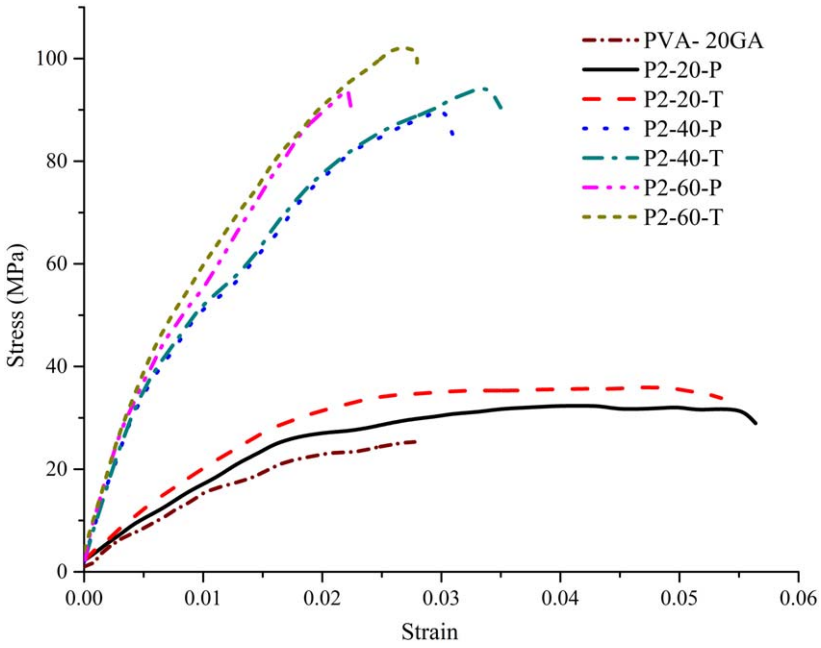


**Figure 14.** Flexural Stress-strain curves of Plain 2 composites for various weight fractions in both warp and weft directions.

### 4.5. Effect of woven structure on mechanical properties

P2 (Plain 2) and WR (Weft Rib) composites are considered to analyze the effect of weaving pattern on tensile, flexural and impact properties. This comparison has been done for the fabrics with same GSM.

#### *4.5.1. Tensile strength*

Increase in fiber weight enhances the tensile properties significantly in both the warp and weft directions. It is observed that tensile properties are better for warp direction compared to the weft direction as seen in figure 15. The ultimate stress increases 9.1 times for warp direction and 7 times for weft direction compared to pure resin case for WR-60 composites. This can be attributed to more number of yarns in warp direction compared to weft direction. Weft yarns are subjected to tearing load and resist more load as compared to deformation. These are two number of yarns in warp direction for every single yarn in weft direction. Another one important factor is higher yarn count associated with the weft compared to the warp direction. Warp and weft direction loading also influences the stress-strain variation as shown in figure 15. For warp direction loading increase in stress is significantly higher than strain in the initial region. Beyond this region, the increase in strain is high compared to

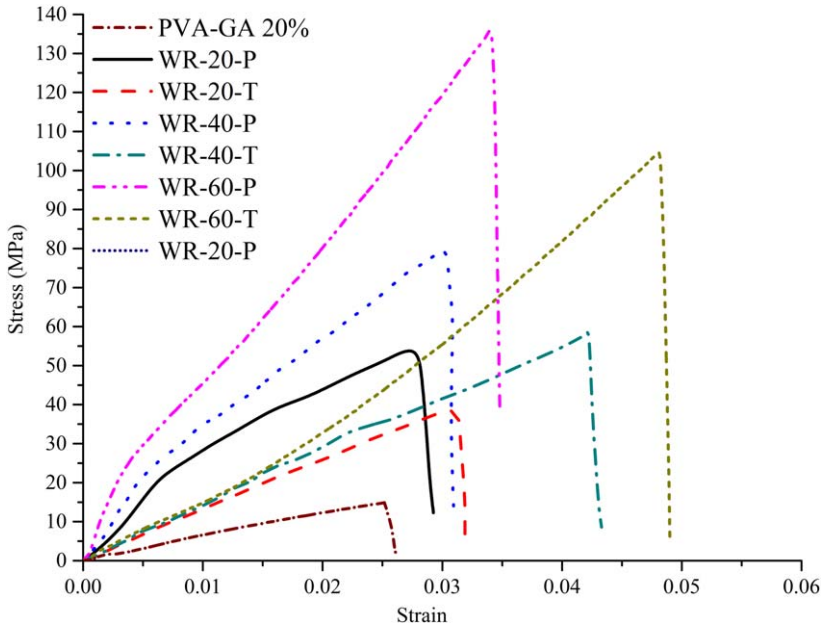


**Figure 15.** Stress-strain diagram of Weft rib composites for various weight fractions under tensile loading.

**Table 5.** Impact strength in J/m$^2$ by various fiber loading of P1, P2 and WR fabric in warp and weft directions.

| Weight % of fabric | 20% fiber | | 40% fiber | | 60% fiber | |
|---|---|---|---|---|---|---|
| Type of woven | Warp (P) | Weft (T) | Warp (P) | Weft (T) | Warp (P) | Weft (T) |
| Plain 1 | 0.8 ± 0.072 | 0.85 ± 0.053 | 1.11 ± 0.068 | 1.23 ± 0.085 | 1.32 ± 0.070 | 1.35 ± 0.086 |
| Plain 2 | 0.95 ± 0.076 | 1.10 ± 0.080 | 1.23 ± 0.058 | 1.35 ± 0.044 | 1.45 ± 0.070 | 1.54 ± 0.046 |
| Weft Rib | 0.94 ± 0.055 | 0.81 ± 0.071 | 1.41 ± 0.147 | 1.12 ± 0.043 | 1.54 ± 0.051 | 1.24 ± 0.086 |

(±) standard deviation for five impact trials.

the stress variation. However, there is no such initial region for the weft loading case and stress-strain increases linearly. This clearly indicates that nature of weaving pattern significantly influences the tensile properties of fabric reinforced composites. The increase in tensile strength in warp direction attributed to shearing of weft yarns leads brittle in nature with moderate strain value. The highest strain with moderate tensile load carrying capacity in weft direction attributed to two weft yarns are subjected to axial loading posses maximum strain value leads to ductile in nature.

*4.5.2. Flexural strength*

P2 and WR composites are considered to analyze the effect of weaving pattern on flexural properties as both are same GSM. Figure 16 clearly shows by adding WR fabric the strain energy absorption decreased, but load carrying capacity increases. This may be attributed that by adding fabric in the composite the bending resistance increases leads to improvement in stress level as compared to strain. For this it can be clearly shows that resin material acts as an elastic member and exhibits very good strain rate with moderate loading ability. By adding fabric ductile fracture of composite converted in to brittle in nature. This may be to due to the yarn linear density of fabric and cover factor is higher than P2. As compared to P2 the loading bearing capacity increases drastically in WR based composites even though both fabrics are having the same GSM. This clearly shows that woven structure or arrange of yarn also having a significant impact on flexural properties.

*4.5.3. Impact strength*

P2 and WR composites are considered to analyze the effect of weaving pattern on impact properties as both fabrics having same GSM. Table 4 it can be observed that Impact strength increases with fiber loading in both warp and weft directions; this attributed more amount of energy absorption by adding fiber to it. But weft direction of composites exhibits lesser impact strength than the warp direction. This clearly shows that yarn liner density and cover factor having a significant effect also on sudden loading.

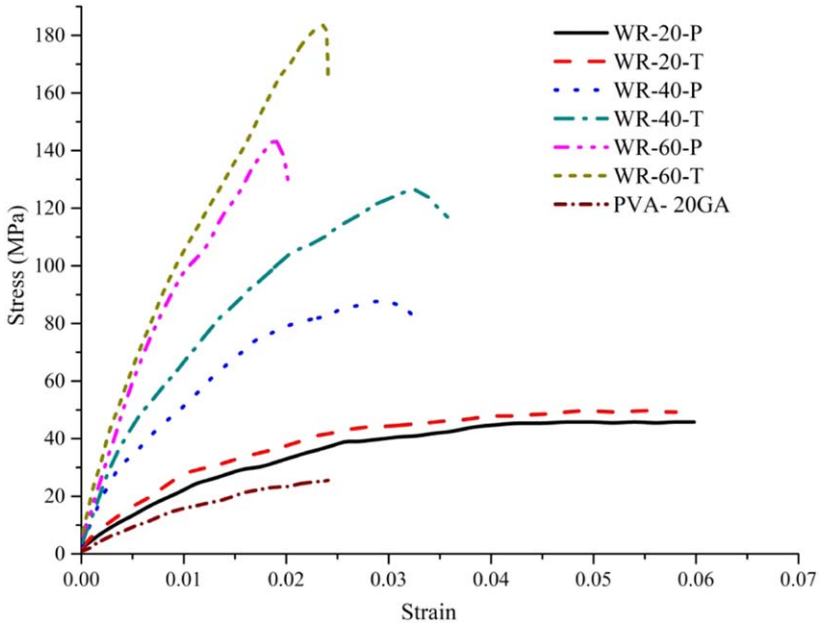


**Figure 16.** Stress-Strain diagram of Weft rib composites for various weight fractions under flexural loading.

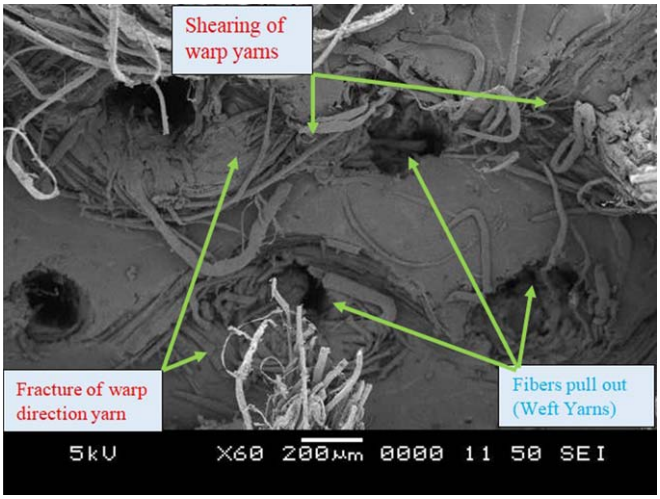


**Figure 17.** SEM image of fractured surface of P1 type of fabric under tensile loading.

### 4.6. Fractured surface analysis

Figure 17 shows the SEM image of fractured surface of tensile specimen. It is evident that fiber pull out failure is happening for the weft yarns while warp yarns are subjected to shearing failure. This clearly indicates that the weft direction yarns are subjected to axial loading as they are aligned along the loading direction and warp direction yarns are subjected to shear loading as they are under tearing loading. This fiber pullout failure along direction leads to the brittle failure of P1 type composite as discussed in section 4.3 (a).

The SEM image of fractured surface of P1 based composites under flexural loading is shown in figure 18. It is clear that bottom layers are subjected to tensile loading which leads to pull out of fibers from the matrix material. The pull out of fiber may be due to the crimp and cover factors, as the crimp increases matrix materials occupies the gap between the two yarns hence it increases the resistance against the bending loading. However, the yarns of top layers are subjected to compression and leads to decrease in the space between the fiber yarns until the yarns come into contact with one another. In other words inter yarn friction resist the slippage of yarn to fiber interface due to crinkles like structure with 'S' type of twist in yarns of woven composites. Also, it clearly shows that the higher percentage of crimp in weft direction allows more amount resin in the curvy regions between the yarns which leads to less amount of strain. Finally, sisal fibers are breaks like sharp cuts which indicates the brittle nature of sisal fiber. This clearly shows that P1 woven fiber composites are withstanding moderate bending loads

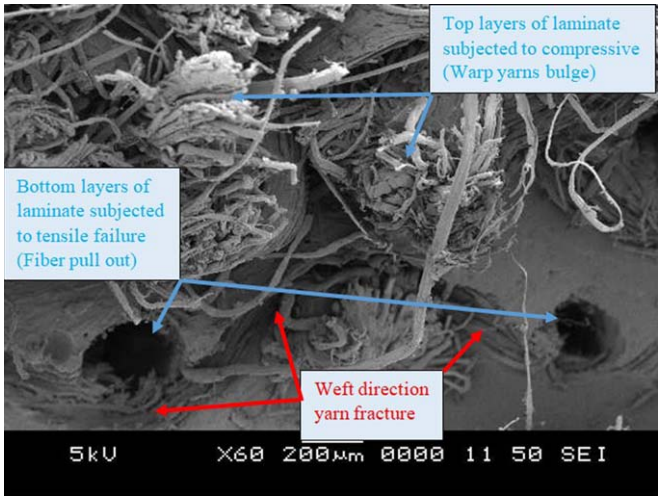


**Figure 18.** SEM image fractured surface of P1 fabric based composites under flexural loading.

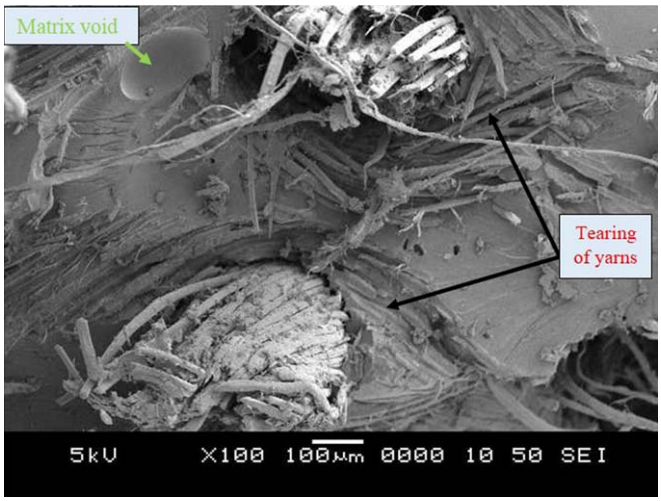


**Figure 19.** SEM image fractured surface of P2 fabric based composites under tensile loading.

with higher strain rate. As the fiber loading increases the pulling capacity increases which results in higher bending strength and higher slipping resistance between the yarns and matrix which results in lesser strain rate.

The SEM image of fractured surface of P2 based composites under tensile loading is shown in figure 19. It shows, pulled-out of yarns, as well as tearing of yarns in many areas, is distinctly observed. Tearing of yarns along the warp direction indicates a good interfacial adhesion between the yarns and matrix. The nature of failure of P2 composites is same as P1 type composites which are brittle failure. The crinkles surface of the yarns increases the resistance to pull and tear the yarn from the matrix material. The resin rich regions are also found along warp directions due to the lower cover factor of the sisal fabric.

The SEM image of fractured surface of P2 based composites under flexural loading is shown in figure 20. It is clearly shows the adhesion between fiber and resin material due to crinkles on the surface of yarn and 'S' type of yarn twist in a fabric. The top layers of the composites are subjected to tensile loading and both pulling and tearing of yarns are observed at higher magnifications. The resin penetration between the gaps of two yarns is also observed. This offers more resistance along the surface of the yarns as discussed in section 4.3(b). However, it depends on cover factor and percentage of crimp in both warp and weft directions.

The SEM image of fractured surface of WR based composites under bending loading is shown in figure 21. As seen in earlier P1 and P2 composites top layers are subjected to compressive loading and bottom layers are subjected to tensile loading, same was observed in WR based composites also. As each warp yarn is crossed with two weft yarns, the strength in weft direction of fabric higher than warp direction of fabric. Due to the presence of two successive yarns on weft direction with less cover factor in warp direction, the warp direction of

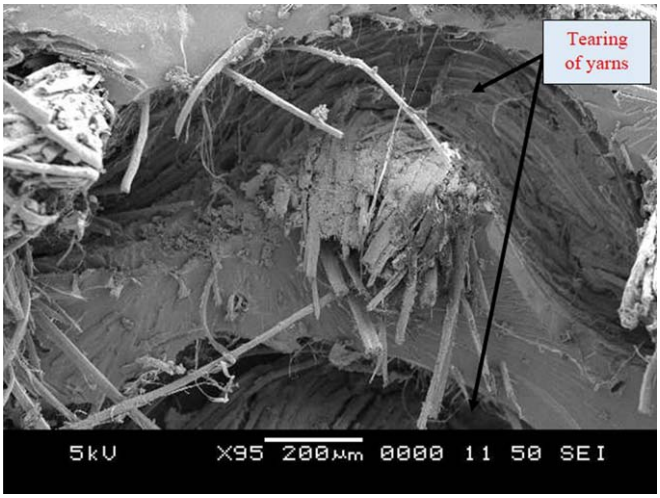


**Figure 20.** Magnified SEM image fractured surface of P2 based composites flexural loading.

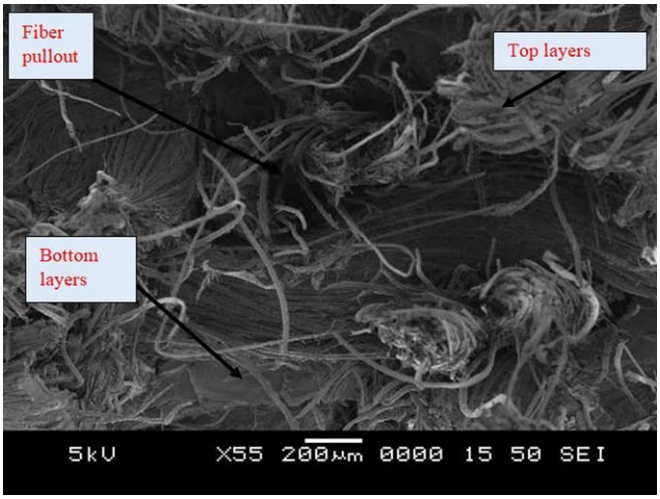


**Figure 21.** SEM image fractured surface of WR based composites under flexural loading.

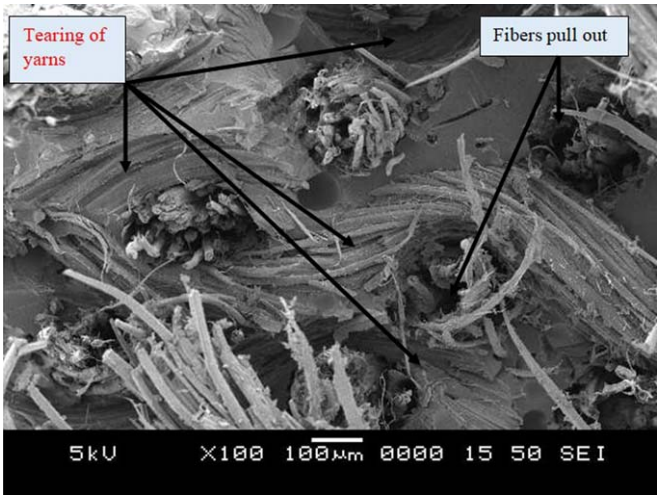


**Figure 22.** SEM image fractured surface of P1 based composites under impact loading.

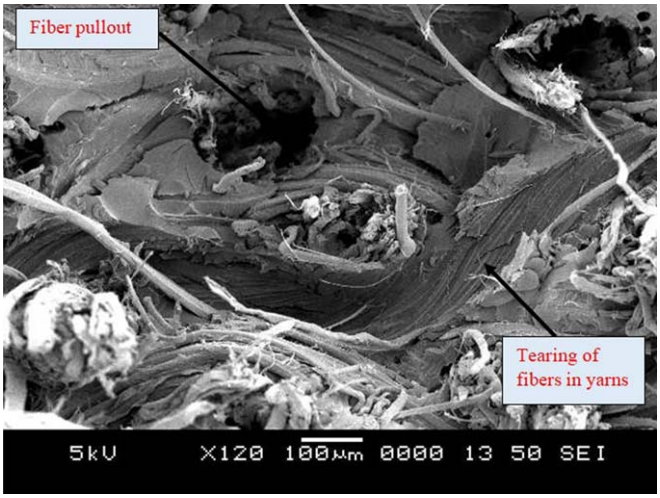


**Figure 23.** SEM image fractured surface of P2 based composites under impact loading.

composite also exhibits batter properties even though yarn liner density and number of yarns are less in warp direction.

The SEM image of fractured surface of P1 based composites under impact loading is shown in figure 22. As yarn linear density is less for warp direction, yarns along warp direction are not transferring the load significantly to the matrix. Figure 22 also reveals that there are no resin rich regions in the fractured surface. It also shows that due to the sudden loading the yarn along the weft direction resists the impact load.

Figure 23 shows the SEM image of fractured surface of P1 based composites under impact loading. In case of P2 the yarn linear density is higher than the P1 so impact load transfer from yarns to resin material and leads to cracks in resin surface. The fibers in yarns are also pulled out, many holes are seen from fractured surface and cracks have been propagated through the resin matrix and presence of river patterns near the fiber surface.

## 5. Conclusions

Mechanical properties of fully biodegradable composites developed from PVA and sisal fabric are analyzed. Influence of weaving architecture, GSM, and fiber loading on different mechanical properties under tensile, flexural and impact loadings. Initially, sisal fabric is characterized for its textile and mechanical properties along warp and weft directions. It is observed that the properties are better along weft direction compared to the warp direction due to the better crimp percentage. It is also observed that all three fabrics are having good range of cover factor which increases the bonding between matrix and fabric material.

Based on the earlier investigation it is found that combination of 80% PVA and 20% GA by weight results in better mechanical properties which is considered for the matrix material. It is observed that P1 and P2 composites have better mechanical properties for weft direction loading compared to warp direction loading. However, for WR composites the properties are better for the loading under warp direction even though yarn linear density is lesser. Mechanical properties of P1 composites are better than the P2 composites due to lower GSM value associated with P1 composites. Similarly, mechanical properties of WR composites are better than P2 composites (for same GSM) due to the woven pattern.

## ORCID iDs

Nagamadhu M https://orcid.org/0000-0001-5996-1955
Jeyaraj P https://orcid.org/0000-0002-8456-8052
G C Mohan Kumar https://orcid.org/0000-0002-7282-7512

## References

[1] Murugan S and Thyla P R 2018 Mechanical and dynamic properties of alternate materials for machine tool structures: a review *J. Reinf. Plast. Compos.* **37** 1456–67
[2] Khan M Z R, Srivastava S K and Gupta M K 2018 Tensile and flexural properties of natural fiber reinforced polymer composites: a review *J. Reinf. Plast. Compos.* **37** 1435–55

[3] Sanjay M R, Madhu P, Jawaid Mohammad, Senthil S and Pradeep S 2018 Characterization and properties of natural fiber polymer composites: a comprehensive review *J. Clean. Prod.* **172** 566–81
[4] Saravana Bavan D and Mohan Kumar G C 2010 Potential use of natural fiber composite materials in India *J. Reinf. Plast. Compos.* **29** 3600–13
[5] Rajesh M and Pitchaimani J 2017 Mechanical characterization of natural fiber intra-ply fabric polymer composites: Influence of chemical modifications *J. Reinf. Plast. Compos.* **36** 1651–64
[6] Ping Tan L T, Steven G P and Ishikawa T 2000 Behavior of 3D orthogonal woven CFRP composites: I. Experimental investigation *Compos. Part A: Appl. Sci. Manuf.* **31** 259–71
[7] Cevallos O A and Olivito R S 2015 Effects of fabric parameters on the tensile behaviour of sustainable cementitious composites *Compos. Part B: Eng.* **69** 256–66
[8] Khan T, Hameed Sultan M T B and Ariffin A H 2018 The challenges of natural fiber in manufacturing, material selection, and technology application: a review *J. Reinf. Plast. Compos.* **37** 770–9
[9] Krivoshapko S N 2018 The perspectives of application of thin-walled plastic and composite polymer shells in civil and industrial architecture *J. Reinf. Plast. Compos.* **37** 217–29
[10] Rajesh M and Pitchaimani J 2016 Dynamic mechanical analysis and free vibration behavior of intra-ply woven natural fiber hybrid polymer composite *J. Reinf. Plast. Compos.* **35** 228–42
[11] Özdemir H and Mert E 2013 The effects of fabric structural parameters on the tensile, bursting and impact strengths of cellular woven fabrics *J. Text Inst.* **104** 330–8
[12] Pothan L A, Mai Y W, Thomas S and Li R K Y 2008 Tensile and flexural behavior of sisal fabric/polyester textile composites prepared by resin transfer molding technique *J. Reinf. Plast. Compos.* **27** 1847–66
[13] Ibrahim I D, Jamiru T, Sadiku E R, Kupolati W K, Agwuncha S C and Ekundayo G 2016 Mechanical properties of sisal fibre-reinforced polymer composites: a review *Compos. Interfaces* **3** 15–36
[14] Sahu P and Gupta M 2017 Sisal (Agave sisalana) fibre and its polymer-based composites: a review on current developments *J. Reinf. Plast. Compos.* **36** 1759–80
[15] Xie Q, Li F, Li J, Wang L, Li Y, Zhang C, Xu J and Chen S 2018 A new biodegradable sisal fiber–starch packing composite with nest structure *Carbohydr. Polym.* **189** 56–64
[16] Abdullah Z W, Dong Y, Davies I J and Barbhuiya S 2017 PVA, PVA blends, and their nanocomposites for biodegradable packaging application *Polym. Plast. Technol. Eng.* **56** 1307–44
[17] Ma Y, Zheng Y, Huang X, Xi T, Lin X, Han D and Song W 2010 Mineralization behavior and interface properties of BG-PVA/bone composite implants in simulated body fluid *Bio. Mater.* **5** 25003
[18] Takasu A, Itou H, Takada M, Inai Y and Hirabayashi T 2002 Accelerated biodegradation of poly (vinyl alcohol) by a glycosidation of the hydroxyl groups *Polym.* **43** 227–31
[19] Gunge A, Koppad P G, Nagamadhu M, Kivade S B and Murthy K V S 2019 Study on mechanical properties of alkali treated plain woven banana fabric reinforced biodegradable composites *Compos. Commun.* **13** 47–51
[20] Saini I, Sharma A, Dhiman R, Ram S and Sharma Pawan K 2017 Structural and thermal characterization of polyvinylalcohol grafted SiC nanocrystals *Mater. Res. Express* **4** 075015
[21] Ramesan M T, Jayakrishnan P, Manojkumar T K and Mathew G 2018 Structural, mechanical and electrical properties biopolymer blend nanocomposites derived from poly (vinyl alcohol)/cashew gum/magnetite *Mater. Res. Express* **5** 015308
[22] Icten B M and Karakuzu R 2008 Effects of weaving density and curing pressure on impact behavior of woven composite plates *J. Reinf. Plast. Compos.* **27** 1083–92
[23] Naik N K, Borade S V, Arya H, Sailendra M and Prabhu S V 2002 Experimental studies on impact behaviour of woven fabric composites: effect of impact parameters *J. Reinf. Plast. Compos.* **21** 1347–62
[24] Senthilkumar K, Saba N, Rajini N, Chandrasekar M, Jawaid M, Siengchin S and Alotman O Y 2018 Mechanical properties evaluation of sisal fibre reinforced polymer composites: a review *Constr. Build. Mater.* **174** 713–29
[25] Samouh Z, Molnar K, Boussu F, Cherkaoui O and Moznine R E 2018 Mechanical and thermal characterization of sisal fiber reinforced polylactic acid composites *Polym. Adv. Technol.* **30** 1–9
[26] Hinterstoisser B and Salmen L 2000 Application of dynamic 2D FTIR to cellulose *Vib. Spectrosc.* **22** 111–8
[27] Glowinska E, Datta J and Parcheta P 2017 Effect of sisal fiber filler on thermal properties of bio-based polyurethane composites *J. Therm. Anal. Calorim.* **130** 113–22
[28] Sathishkumar T P, Naveethakrishnan P, Shankar S, Rajesekar R and Rajini N 2013 Characterization of natural fiber and composites—a review *J. Reinf. Plast. Compos.* **32** 1457–76
[29] Molki B, Heidarian P, Aframehr W M, Nasri-Nasrabadi B, Bahrami B, Ahmadi M, Komeily-Nia Z and Bagheri R 2019 Properties investigation of polyvinyl alcohol barrier films reinforced by calcium carbonate nanoparticles *Mater. Res. Express* **6** 055311
[30] Yar M, Masood A, Batool R, Shahzadi L, Khan A F, Yousaf Z, Rafique M Y and Razaq A 2019 Nano $MnO_2$ immobilized covalently cross-linked chitosan and PVA based highly flexible membranes *Mater. Res. Express* **6** 085055
[31] Madhuri S N and Rukmani K 2019 Synthesis and concentration dependent tuning of PVA-$Sm_2O_3$ nanocomposite films for optoelectronic applications *Mater. Res. Express* **6** 075017
[32] Chen G, Ding X and Progress B 2006 Simulation and strength prediction of woven fabric under uni-axial tensile loading *Text Res. J.* **76** 875–82
[33] Joseph P V, Joseph K and Thomas S 2002 Short sisal fiber reinforced polypropylene composites: the role of interface modification on ultimate properties *Compos Interface* **9** 171–205
[34] Głowin´Ska E, Datta J and Parcheta P 2017 Effect of sisal fiber filler on thermal properties of bio-based polyurethane composites *J. Therm. Anal. Calorim.* **130** 113–22
[35] Patil N V, Rahman M M and Netravali A N 2017 'Green' composites using bioresins from agro-wastes and modified sisal fibers *Polym. Compos.* **40** 99–108
[36] Asha Krishnan K, Jose C, Rohith K R and George K E 2015 Sisal nanofibril reinforced polypropylene/polystyrene blends: morphology, mechanical, dynamic mechanical and water transmission studies *Ind. Crop. Prod.* **71** 173–84
[37] Karthikeyan R, Tjong J, Sanjay K and Sain M M 2017 Mechanical properties and cross-linking denscity of short sisal fiber reinforced silicone composites *Bio. Res.* **12** 211–27
[38] Mani M P and Jaganathan S K 2018 Blood compatibility assessments of novel electrospun PVA/egg white nanocomposite membrane *Bioinspir. Biomim. Nan.* **7** 213–8
[39] Nasikhudin, Ismaya E P, Diantoro M, Kusumaatmaja A and Triyana K 2017 Preparation of PVA/$TiO_2$ composites nanofibers by using electrospinning method for photocatalytic degradation *IOP Conference Series: Mater. Sci. Eng.* **202** 012011

[40] Trohotri M, Jain D, Dwivedi U K, Khan F H, Malik M M and Qureshi M S 2013 Effect of silver coating on electrical properties sisal fiber epoxy composites *Polym. Bull.* **70** 3501–17
[41] Khan M A, Guru S, Padmakaran P, Mishra D, Mudgal M and Dhakad S 2012 Characterisation studies and impact of chemical treatment on mechanical properties of sisal fiber *Compos Interface* **18** 527–41
[42] Sreekumar P A, Saiah R, Saiter J M, Leblanc N, Joseph K, Unnikrishnan G and Thomas S 2009 Dynamic mechanical properties of sisal fiber reinforced polyester composites fabricated by resin transfer molding *Polym. Compos.* **30** 768–75
[43] Maya Jacob S T and Varughese K T 2006 Novel woven sisal fabric reinforced natural rubber composites: tensile and swelling characteristics *J. Compos. Mater.* **40** 1471–85
[44] Fávaro S L, Ganzerli T A, de Carvalho Neto A G V, da Silva O R R F and Radovanovic E 2010 Chemical, morphological and mechanical analysis of sisal fiber-reinforced recycled high-density polyethylene composites *Express Polym. Lett.* **4** 465–73
[45] Xavier F D, Bezerra G S, Santos S F M, Oliveira L S C, Silva F L H, Silva A J O and Conceição M M 2018 Evaluation of the simultaneous production of xylitol and ethanol from sisal fiber *Biomolecules* **8** 1–13
[46] Misnon M I, Islam M M, Epaarachchi J A and Lau K T 2015 Analyses of woven hemp fabric characteristics for composite reinforcement *Mater. Des.* **66** 82–92
[47] Mohan Kumar G C, Jeyaraj P and Nagamadhu M 2019 Dynamic mechanical analysis of glutaraldehyde cross linked polyvinyl alcohol under tensile mode *AIP Conf. Proc.* **020017** 2057
[48] Zhanying S and Wu M 2019 Effects of sol-gel modification on the interfacial and mechanical properties of sisal fiber reinforced polypropylene composites *Industrial Crops & Products* **137** 89–97
[49] Pappu A, Pickering K L and Thakur V K 2019 Manufacturing and characterization of sustainable hybrid composites using sisal and hemp fibres as reinforcement of poly (lactic acid) via injection moulding *Ind. Crop. Prod.* **137** 260–9
[50] Chaitanya S, Singh I and Sing J I 2019 Recyclability analysis of PLA/Sisal fiber bio-composites *Compos Part B* **173** 106895
[51] Hari R and Mini K M 2019 Mechancial and Durability properties of sisal-nylon 6 hydrid fiber reinforced high strength SCC *Contr. Build Mater.* **204** 479–91
[52] Milanese A C, Cioffi M O H and Voorwald H J C 2012 Thermal and mechanical behavior of sisal/phenolic composites *Compos Part B* **43** 2843–50